Double Pair Production by Ultra High Energy Cosmic Ray Photons

S.V. Demidov* **and O.E. Kalashev***

**Institute for Nuclear Research of the Russian Academy of Sciences,*
60th October Anniversary Prospect 7a, Moscow 117312 Russia

Abstract. **With use of CompHEP package we've made the detailed estimate of the influence of double e^+e^- pair production (DPP) by photons on the propagation of ultra high energy electromagnetic (EM) cascade. We show that in the models in which cosmic ray photons energy reaches few$\times10^3$ EeV refined DPP analysis may lead to substantial difference in predicted photon spectrum compared to previous rough estimates.**

Keywords: **Double Pair Production**

I. INTRODUCTION

Ultra-high energy (UHE) photons have not been recognized so far by any of present generation experiments [1], [2], [3], [4], although their existence is predicted by Greisen–Zatsepin–Kuzmin effect [5], [6] as well as by most of hypothetical top-down models of UHE cosmic rays origin. There are several bounds on fraction and flux of ultra-high energy photons above $10-100$ EeV obtained by independent experiments [7], [8], [9]. Photon limits are used to constrain the parameters of top-down models (see for example [10]). Understanding interactions of UHE photons with universal backgrounds is a crucial point for building such constraints.

In the wide energy range the spectra of electron and photon components of cosmic rays follow each other due to relatively rapid processes transferring γ-rays to electrons and backwards. Pair production (PP) and inverse Compton scattering (ICS) are the main processes that drive the EM cascade. In the Klein–Nishina limit where $s \gg m_e^2$, either electron or positron produced in a pair production event typically carries almost all of the initial total energy. The produced electron (positron) then undergoes ICS losing more than 90 % of energy and finally the background photon carries away almost all of the initial energy of the UHE photon. Due to this cycle the energy loss rate of the leading particle in the EM cascade is more than one order of magnitude less than interaction rate. However in presence of a random extragalactic magnetic field (EGMF) the electrons may lose substantial part of their energy by emitting synchrotron radiation. In this case, starting from certain energy the synchrotron loss rate for the electrons becomes to dominate over ICS rate, which leads to suppression of the EM cascade development. Its penetration depth is then defined by the photon mean free path. Depending on the value of EGMF this transition may occur between ~ 1 EeV and $\sim 10^6$ EeV.

In this article we consider higher order process, double e^+e^- pair production (DPP) by photons. The DPP cross section grows rapidly with s near the threshold and quickly approaches the asymptotic value $\sigma(\infty) \simeq 6.45$ μb [11], [12], [13]. The explicit energy dependence of the DPP cross section was estimated in Ref. [14] by calculating the dominant contribution from two e^+e^- pairs to the absorptive part of gamma-gamma forward scattering amplitude. Since PP cross section decreases with the increase of $\sqrt{s}$ the DPP rate starts to dominate over PP rate above certain energy. For interactions with CMB the transition occurs above ~ 1000 EeV. In presence of the radio background this energy goes up somewhat. If the EGMF is less than 10^{-11} G the EM cascade still exists at these energies and one should accurately count the secondary electrons from DPP. So far the EM cascade simulations such as [15], [16] roughly estimated DPP effect by utilizing the total cross section and assuming that one e^+e^- pair of the two carries all the initial energy while two particles in the pair are produced with the same energy. By making use of CompHEP package [17], [18], [19] we numerically calculate differential cross section for DPP and compare the influence of DPP on propagation of ultra high energy EM cascade with previous estimates.

The paper is organized as follows. In Sec. II we present the results of the calculation of DPP cross section. In Sec. III we illustrate the influence of DPP in model example. In Sec. IV we summarize our results.

II. DPP CROSS SECTION CALCULATION

As it was mentioned in the Introduction the DPP process begins to dominate over PP at very high energies $E_\gamma \gtrsim 1000$ EeV or $s \gtrsim 1$ GeV^2, which is well beyond the DPP threshold. At these and higher energies DPP has noticeable effect on the propagation of EM cascade. In this energy region DPP total cross section is practically saturated by its asymptotic value. So, we are interested here mostly in energy and angular distributions of secondary electrons (positrons) in asymptotic regime $(s \to \infty)$.

We use CompHEP package for calculation of tree level differential DPP cross sections. This package allows to perform automatic calculations of matrix elements and their squares for any process $2 \to 2, .., 2 \to 4$ at tree level. Then, with the aid of CompHEP one can integrate squared matrix elements over selected part of multi-particle phase space. See Refs. [17], [18], [19] for the details.

We introduce binning in the energy E^* of one of the produced electrons[1]. Then we perform CompHEP simulations in the centre of mass frame (CMF) and obtain distributions over $\cos\Theta^*$ of the cross section in a given energy bin. Here Θ^* is the angle between the collision axis and the momentum vector of the electron.

These calculations show that the angular distribution of secondaries tends to a strongly peaked function of $\cos\Theta^*$ in the asymptotic energy range. The peaks are located at forward and backward directions, i.e. at $\cos\Theta^* = \pm 1$. This behavior is illustrated by Fig. 1 where we show an example of angular distribution for
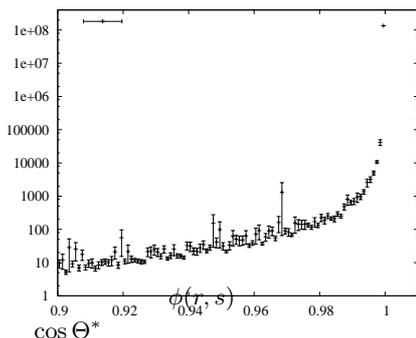

Fig. 1: Example of distribution of the DPP cross sections over $\cos\Theta^*$ for $\sqrt{s} = 10.0$ GeV in energy E^* bin $2.25 - 2.5$ GeV.

$\sqrt{s} = 10.0$ GeV. The effect that most of secondaries go forward or backward becomes more pronounced with the increase of $\sqrt{s}$ and in the case of fixed $\sqrt{s}$ with higher energy E^* of electron. Numerically we found that the probability of emitting secondary electron inside the cone with $|1 - \cos\Theta^*| < 1/50$ is 96.8% for $\sqrt{s} = 1.0$ GeV, 98.7% for $\sqrt{s} = 2.5$ GeV and 99.6% for $\sqrt{s} = 10.0$ GeV. Also we checked that the probability of producing two forward secondaries of the same type (e.g., when both forward particles are electrons) integrated over energies and directions of other secondaries, is of order 10^{-3}. So, the main part of events consists of two e^+e^- pairs going to the opposite directions along the collision axis.

Let us now turn to the energy distribution. It is clear from the symmetry of the problem that the energy distribution in the CMF frame should be the same for the forward and backward electrons. Let us write the DPP differential cross section in the form

$$\frac{d\sigma}{dE^*} \equiv \frac{1}{\sqrt{s}} \phi\left(\frac{E^*}{\sqrt{s}/2}, s\right) \sigma_{tot}(s) \,. \qquad (1)$$

Then the energy conservation condition gives

$$\sqrt{s}\sigma_{tot}(s) = 4 \int_0^{\sqrt{s}/2} E^* \frac{d\sigma}{dE^*} \, dE^* = \qquad (2)$$

---

[1] Here and further we denote by "*" quantities measured in the center of mass frame.

$$= \sigma_{tot}(s) \sqrt{s} \int_0^1 r\phi(r, s) \, dr$$

or for any value of s

$$\int_0^1 r\phi(r, s) \, dr = 1 \,. \qquad (3)$$

Imposing probability conservation requirement

$$\sigma_{tot}(s) = \int_0^{\sqrt{s}/2} \frac{d\sigma}{dE^*} \, dE^* \qquad (4)$$

gives another integral constraint on $\phi(r, s)$:

$$\int_0^1 \phi(r, s) \, dr = 2 \,. \qquad (5)$$

Although conditions (3) and (5) do not necessary imply $d\phi/ds = 0$ the results of CompHEP simulations show that for large enough s, when cross section approaches its asymptotic value, the energy distribution of secondaries in units of maximal energy $\sqrt{s}/2$ varies only slightly with $\sqrt{s}$. In Fig. 2 we plot the distribution
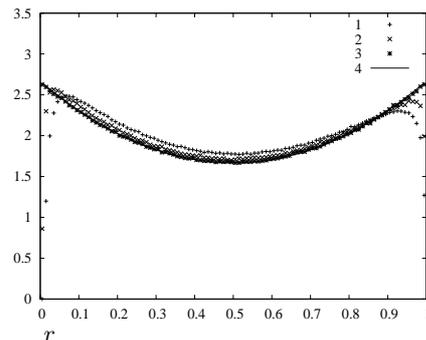

Fig. 2: The normalized energy distributions $\phi(r, s)$, $r = 2E^*/\sqrt{s}$ (see main text for details): 1) $\sqrt{s} = 0.1$ GeV, 2) $\sqrt{s} = 0.25$ GeV, 3) $\sqrt{s} = 10.0$ GeV and 4) the analytic approximation Eq. (6).

$\phi(r, s)$ as a function of r for different values of $\sqrt{s}$. One can see that with varying $\sqrt{s}$ the only changes in these distributions are concentrated at the borders of the plot. The distribution limit for $s \to \infty$ can be fitted (see fig. 2) by simple analytic expression, which satisfies constraints (3) and (5),

$$\phi_{fit}(r) = \frac{5}{3} + (2r - 1)^2. \qquad (6)$$

For comparison, the earlier approximation [15], [16] in terms of the distribution $\phi(r, s)$ reads

$$\phi(r, s) = 2 \cdot \delta(r - 0.5). \qquad (7)$$

In our further calculations we use for the energy distribution the Eq. (1), where $\phi(r, s) = \phi_{fit}(r)$ is given by Eq. (6) and assume that all the secondary particles are directed alongside the collision axis. In Sec. III we discuss how good the above approximation is.

III. MODEL EXAMPLE

In the previous section we have found the precise expression for the distribution of secondary electrons from DPP. Here we consider a model example to illustrate the difference introduced by the specified cross section compared to the previous estimates.

We use a numerical code developed in Ref. [15] to compute the flux of produced photons and protons. The code is based on the transport equations and calculates the propagation of nucleons, electrons and photons using the dominant processes. For EM cascade it includes all the processes mentioned above. For nucleons, it takes into account single and multiple pion production and e^+e^- pair production, neutron β-decay. The propagation of nucleons and the EM cascades are calculated self-consistently, that is secondary particles produced in all reactions are propagated alongside the primaries. For the details on the calculation of the ransport equation coefficients see Ref. [20]:

Besides CMB the radio, infra-red and optical (IRO) components of the universal photon background are taken into account in the simulation. Note that the radio background is not yet well known. Our results will depend strongly on the radio background assumed. Three models considered in this work are estimates by Clark *et al.* [21] and the two models of Protheroe and Biermann [22], both predicting larger background than the first one. For the IRO background component we used the model [23]. This component doesn't have substantial effect on the propagation of UHE protons and EM cascade. For the strength of the random extragalactic magnetic field we use the range of values 10^{-12}G $< B < 10^{-11}$G following the estimate [24].

Among the models we have chosen the one in which the UHE photons contribute substantial part of the total spectrum. Note that such models are strictly limited by the present experimental bounds on the photon component, see [10] for details.

In Fig. 3 the propagated cosmic ray flux is shown for proton sources with spectrum

$$\frac{d\Phi}{dE} \sim E^{-1.5}, \ E < 10^4 \text{EeV} \tag{8}$$

homogeneously distributed in the Universe and having no evolution in the comoving frame. The spectrum presented is normalized on HiRes [3] results (fitting was done above 40 EeV). The solid line represents the total UHE cosmic ray flux calculated with use of new DPP estimate. The dotted line shows proton component. The dashed line shows total flux calculated using earlier DPP estimate (Eq. 7), utilizing the total cross section and assuming that one e^+e^- pair of the two carries all the initial energy while two particles in the pair are produced with the same energy. The dash-dotted lines are built without taking DPP into account at all.

It is clear from the Fig. 3 that DPP suppresses γ ray flux above 100 EeV. This is only true if the minimal radio background model [21] is used. The same picture
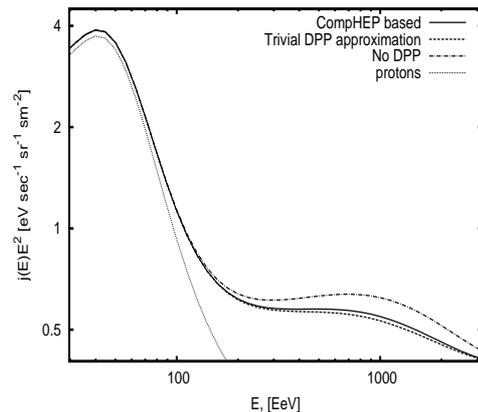

Fig. 3: Fluxes predicted by proton emitting source described in text. The dotted line represents proton component, while solid, dashed and dash-dotted lines represent total flux calculated with CompHEP based DPP, trivial DPP estimate and without DPP correspondingly.

made for any of the two models of [22] haven't shown any effect of DPP, since in this case the γ flux is strongly suppressed by PP on radio. Increasing magnetic field above 10^{-11}G also destroys the picture, this time due to synchrotron radiation. In the case of minimal radio background and moderate EGMF the trivial DPP effect estimate leads to extra suppression compared to the more accurate one proposed in this paper. Although overall error in terms of integral photon flux above 100 EeV turns to be only $+7\%$ for the curve disregarding DPP and just -1.5% for the trivial DPP estimate. Note that integral photon flux fraction predicted in this model is 34%, which is very close to the upper bound [7]. So
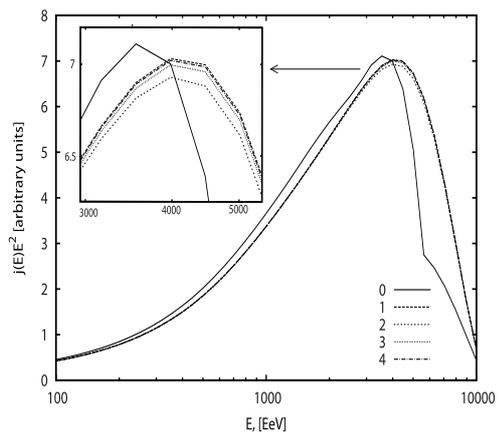

Fig. 4: Electron flux predicted by photon emitting source described in text using 0) earlier estimate Eq. (7); 1) analytical fit (6); 2) analytical fit (6) + 3.2% perpendicular component (see details in text); 3) $\phi(r, 1 \, \text{GeV}^2)$; 4) $\phi(r, 100 \, \text{GeV}^2)$.

far we used the fixed energy distribution (6) for all values of s. Also we assumed that all the secondary particles are directed alongside the collision axis. Let

us now check how accurate the above approximations are. We have repeated our simulations replacing the energy distribution (6) by the tabulated functions obtained with use of CompHEP for $\sqrt{s} = 1\,\mathrm{GeV}$ and $\sqrt{s} = 10\,\mathrm{GeV}$. To see the maximal possible effect of the nontrivial angular distribution of secondaries we have also repeated our calculations assuming that 3.2% of secondary particles are aligned perpendicular to the collision axis in the CMF, while the rest of the particles are directed alongside the axis. We don't show here the modified fluxes obtained in the model corresponding to Fig. 3, since they are practically indistinguishable from the curves already shown. Instead to illustrate the maximal possible error introduced by the approximation used, here we consider the pure photon sources with the same injection spectrum (8) as in Fig. 3 and count the income to the propagated electron and photon spectra from the uniformly distributed sources located within $500\,\mathrm{Mpc}$ from the observer. In Figs. 4 and 5 the electron and photon fluxes in this model are shown respectively. Also on these figures the fluxes calculated using earlier
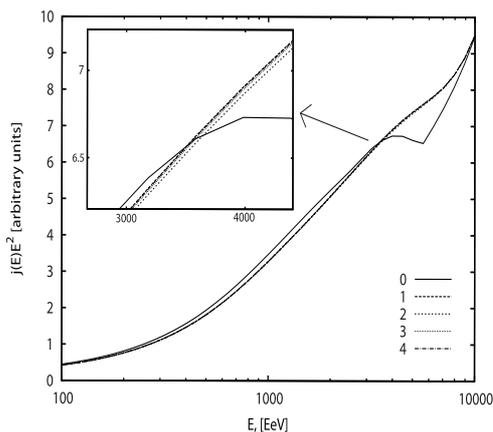

Fig. 5: Propagated photons flux predicted by photon emitting source described in text. The designation of curves is the same as on Fig. 4.

estimate Eq. (7) are shown. From the figures it is clear that the earlier estimate may lead to the artificial features in the spectra which doesn't appear in our analysis. Also it is clear that discrepancy between the curves 1-4 representing different variants of our analysis are small compared to the error introduced by the earlier estimate. In fact the difference between the curves 1-4 is comparable to the error introduced by finite energy binning used in our numerical code.

IV. CONCLUSION

In this work we have considered in detail the DPP process. We have estimated the distribution of secondary electrons and positrons and made the improved cosmic rays simulation based on the new estimate. We have shown that in certain cases the DPP process may modify the photon component of the spectrum substantially. However this modification can only be seen if radio

background is close to the minimal model [21] and EGMF is lower than $10^{-11}\mathrm{G}$. In this case there is an energy range where DPP is the main attenuation mechanism for γ rays and therefore differences in DPP estimates can clearly be seen. Although in the vast majority of the models which do not contradict to the present experimental bounds on the photon fraction in UHE cosmic rays DPP process doesn't make a substantial contribution to the attenuation and therefore can be treated simplistically or even disregarded.

REFERENCES

[1] M. Takeda *et al.*, Astropart. Phys. **19**, 447 (2003) [arXiv:astro-ph/0209422].
[2] V. P. Egorova *et al.*, Nucl. Phys. Proc. Suppl. **136**, 3 (2004) [arXiv:astro-ph/0408493].
[3] R. U. Abbasi *et al.* [High Resolution Fly's Eye Collaboration], Phys. Rev. Lett. **92**, 151101 (2004) [arXiv:astro-ph/0208243].
[4] J. Abraham *et al.* [Pierre Auger Collaboration], Phys. Rev. Lett. **101**, 061101 (2008) [arXiv:0806.4302 [astro-ph]].
[5] K. Griesen, Phys. Rev. Lett. **16**, 748 (1966)
[6] Z. T. Zatsepin and V. A. Kuz'min, Zh. Eksp. Teor. Fiz. Pis'ma Red. **4**, 144 (1966)
[7] G. I. Rubtsov *et al.*, Phys. Rev. D **73**, 063009 (2006) [arXiv:astro-ph/0601449].
[8] A. V. Glushkov, D. S. Gorbunov, I. T. Makarov, M. I. Pravdin, G. I. Rubtsov, I. E. Sleptsov and S. V. Troitsky, JETP Lett. **85**, 131 (2007) [arXiv:astro-ph/0701245].
[9] J. Abraham *et al.* [Pierre Auger Collaboration], Astropart. Phys. **29**, 243 (2008) [arXiv:0712.1147 [astro-ph]].
[10] G. Gelmini, O. Kalashev and D. V. Semikoz, J. Exp. Theor. Phys. **106**, 1061 (2008) [arXiv:astro-ph/0506128].
[11] H. Cheng and T. T. Wu, Phys. Rev. D **1** (1970) 3414.
[12] H. Cheng and T. T. Wu, Phys. Rev. D **2** (1970) 2103.
[13] L. N. Lipatov and G. V. Erolov, Yad. Fiz. **13** (1971) 588.
[14] R. W. Brown *et al.*, Phys. Rev. D **8**, 3083 (1973).
[15] O.E. Kalashev, V.A. Kuzmin and D.V. Semikoz, [arXiv:astro-ph/9911035]. O.E. Kalashev Ph.D. Thesis, INR RAS, 2003. G. B. Gelmini, O. Kalashev and D. V. Semikoz, JCAP **0711**, 002 (2007) [arXiv:0706.2181 [astro-ph]].
[16] S. Lee, Phys. Rev. D **58**, 043004 (1998) [arXiv:astro-ph/9604098].
[17] E. Boos *et al.* [CompHEP Collaboration], Nucl. Instrum. Meth. A **534** (2004) 250 [arXiv:hep-ph/0403113].
[18] A. Pukhov *et al.*, arXiv:hep-ph/9908288.
[19] http://comphep.sinp.msu.ru
[20] S. V. Demidov and O. E. Kalashev, arXiv:0812.0859 [astro-ph].
[21] T. A. Clark, L. W. Brown, and J. K. Alexander, Nature **228**, 847 (1970).
[22] R. J. Protheroe and P. L. Biermann, Astropart. Phys. **6**, 45 (1996) [Erratum-ibid. **7**, 181 (1997)]
[23] F. W. Stecker, M. A. Malkan and S. T. Scully, Astrophys. J. **648**, 774 (2006).
[24] K. Dolag, D. Grasso, V. Springel and I. Tkachev, JETP Lett. **79**, 583 (2004) [Pisma Zh. Eksp. Teor. Fiz. **79**, 719 (2004)]; and JCAP **0501**, 009 (2005).